Current Biology 24, 2708–2713, November 17, 2014 ©2014 Elsevier Ltd All rights reserved http://dx.doi.org/10.1016/j.cub.2014.09.053

Report

Augmin Triggers Microtubule-Dependent Microtubule Nucleation in Interphase Plant Cells

Ting Liu,[1,2,4] Juan Tian,[1,4] Guangda Wang,[1,2,4] Yanjun Yu,[1] Chaofeng Wang,[1,2] Yinping Ma,[1,2] Xiaxia Zhang,[1,2] Guixian Xia,[1] Bo Liu,[3] and Zhaosheng Kong[1,*]

[1]State Key Laboratory of Plant Genomics, Institute of Microbiology, Chinese Academy of Sciences, Beijing 100101, China

[2]University of Chinese Academy of Sciences, Beijing 100049, China

[3]Department of Plant Biology, University of California, Davis, CA 95616, USA

Summary

Microtubule (MT)-dependent MT nucleation by γ-tubulin is required for interphase plant cells to establish a highly dynamic cortical MT network underneath the plasma membrane, which influences the deposition of cell wall materials and consequently governs patterns of directional cell expansion [1–6]. Newly formed MTs either assume 40° angles or are parallel to the extant ones [7–9]. To date, it has been enigmatic how the γ-tubulin complex is recruited to the sidewall of cortical MTs and initiates MT nucleation [10]. Here, we discovered that the augmin complex was recruited to cortical MTs and initiated MT nucleation in both branching and parallel forms. The augmin complex overwhelmingly colocalized with the γ-tubulin complex. When the function of the augmin complex was compromised, MT nucleation frequency was drastically reduced, most obviously for the branching nucleation. Consequently, the augmin knockdown cells displayed highly parallel and bundled MTs, replacing the fine and mesh-like MT network in the wild-type cells. Our findings uncovered a mechanism by which the augmin complex functions in recruiting the γ-tubulin complex to cortical MTs and initiating MT nucleation, and they shifted the paradigm of the commonly perceived mitotic-specific function of augmin and established its crucial function in MT-dependent MT nucleation in interphase plant cells.

Results and Discussion

The Augmin Complex Is Recruited to Cortical MTs and Initiates Both Branching and Parallel MT Nucleation

The augmin complex plays a critical role in mitotic spindle assembly by generating short and dense intraspindle microtubules (MTs) in both animal and plant cells [11–16]. The current model is that the augmin complex binds to MT walls and recruits the γ-tubulin ring complex (γTuRC) via the WD40 repeat protein NEDD1 to initiate new MT nucleation [13, 17–20]. MT-dependent MT nucleation by γTuRC in interphase cells has been well characterized by live-cell imaging in plants [8, 21]. However, it is still undetermined whether the augmin complex is involved in the regulation of γTuRC-dependent MT nucleation in interphase plant cells.

To determine whether the augmin complex is associated with the interphase cortical MTs, we performed live-cell imaging using the conserved subunit AUG3 [15] and a plant-specific subunit AUG7 [16] as the reporter. We recorded both AUG3/7-GFP and the cortical MTs labeled by mCherry-TUB6 in the interphase pavement cells on the *Arabidopsis* leaf epidermis. Notably, both AUG3-GFP and AUG7-GFP decorated the cortical MTs and appeared as discrete particles that remained immobile for different lengths of time before disappearing from the cortical MTs (Figures S1A and S1B available online; Movie S1). Persistent residence of AUG3/7-GFP usually led to new MT initiations, either in the branching form or in the parallel form (Figures 1A–1C; Figure S2A; Movie S1). Importantly, these results revealed that augmin was associated with MT nucleation in interphase cells.

Interestingly, we found a small portion of augmin-associated MT nucleation events taking place at the MT crossover sites. Following the recruitment of augmin particles to the newly formed MT crossover sites, a fraction of them subsequently led to MT nucleation, either in the branching form or in the parallel form along the preexisting MTs (Figure S3A; Movies S1 and S2). This finding is consistent with the published observation of MT initiation at the crossover sites in *Arabidopsis* hypocotyl epidermal cells using EB1a-GFP and GFP-TUB6 as the markers [9]. However, it was still uncertain whether MT nucleators, like the γTuRC, were implicated in this process. Thus, we examined γTuRC dynamics (Figure S1C; Movie S1) in leaf epidermal pavement cells, using the GCP2-3xGFP fusion [8] as the reference. Similar to augmin, a small portion of GCP2-3xGFP particles were also recruited to the MT crossover points, and a fraction of them subsequently led to new MT growth (Figure S3B; Movie S2). Together, the results firmly indicate that augmin-associated MT initiation at MT crossover sites was a bona fide MT nucleation event coupled with the γTuRC.

Augmin Is Specifically Associated with MT-dependent MT Nucleation

To further gain insights into the function of augmin in the assembly of interphase MTs, we tracked 522 AUG3-GFP particles in six cells of three seedlings, 627 AUG7-GFP particles in seven cells of four seedlings, and 492 GCP2-3xGFP particles in four cells of three seedlings. We assessed the relationship between the appearance of augmin/γTuRC on cortical MTs and the dynamic behaviors of cortical MTs at the site and divided them into five categories, with the augmin/γTuRC-associated MT nucleation at crossovers incorporated into the categories of either branching or parallel nucleation (Figure 1D). In general, augmin exhibited a similar dynamic pattern to that of the MT-associated GCP2-3xGFP, with approximately one half of the AUG3/7-GFP particles appearing transiently on the cortical MTs (type 1 in Figure 1D) without initiating MT nucleation. The remaining half resided persistently on the MTs and subsequently led to MT nucleation, more frequently in the branching form (type 2 in Figure 1D) than in the parallel form (type 3 in Figure 1D). However, 7.35% of GCP2-3xGFP particles appeared at the cell cortex devoid of MTs (types 4 and 5 in Figure 1D), and about one-fifth

[4]Co-first author

*Correspondence: zskong@im.ac.cn

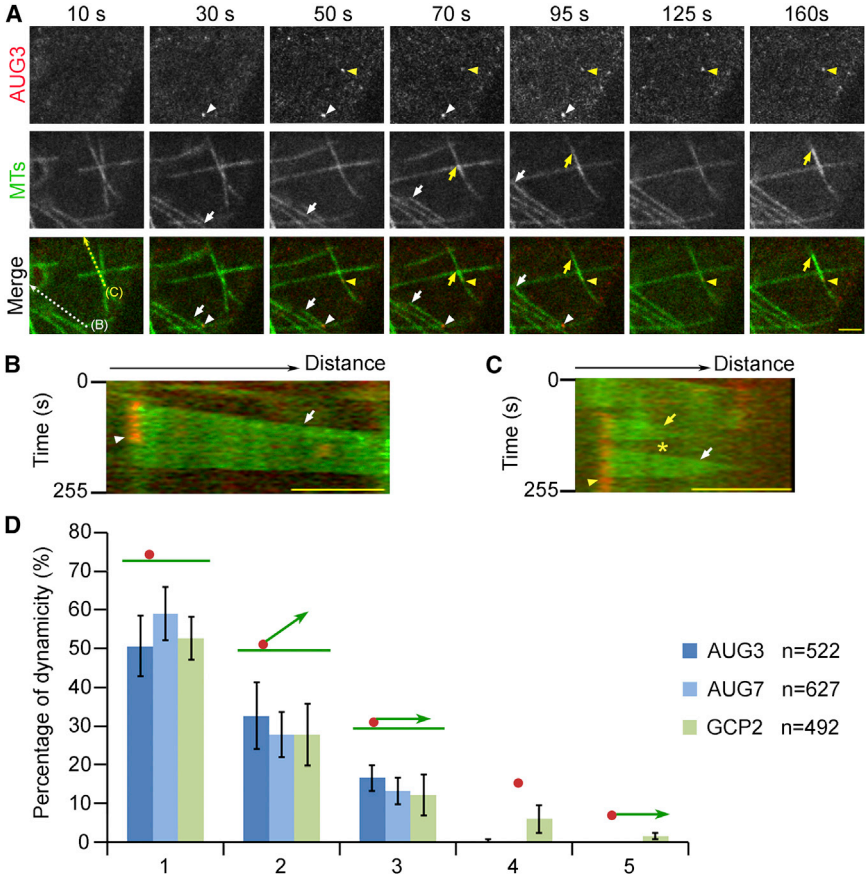

Figure 1. Augmin-Associated MT-Dependent MT Nucleation in Epidermal Pavement Cells

(A) Time-lapsed images showing AUG3-associated MT nucleation events. In the merged images, AUG3-GFP is pseudocolored in red, and MTs are pseudocolored in green. White arrowheads indicate an AUG3-GFP particle associated with a branching nucleation event, with the growing plus end of the nascent MT tracked by white arrows. The dashed white arrow along the trajectory of the nascent MT highlights the area and the direction for kymograph analysis of the branching nucleation event in (B). Yellow arrowheads indicate an AUG3-GFP particle associated with a parallel nucleation event, with the growing plus end of the nascent MT tracked by yellow arrows. The nascent MT was depolymerized, and another parallel nucleation event was initiated from the same AUG3-GFP particle. The dashed yellow arrow along the nascent MT highlights the area and the direction for kymograph analysis of the parallel events (C). The scale bar represents 2 μm. See also Movie S1.

(B) Kymograph showing a daughter MT initiated from an AUG3-GFP particle and then branched off of the mother MT. The green slope indicated by the white arrow illustrates the growth of the nascent MT, and the red line indicated by the white arrowhead shows the persistent residence of the AUG3-GFP. The scale bar represents 2 μm.

(C) Kymograph showing two successive parallel MT nucleation events that were initiated from an AUG3-GFP particle. The overlaid green slope indicated by the yellow arrow illustrates growth of the nascent MT. The overlaid green slope indicated by the white arrow illustrates the successive nascent MT initiated from the same AUG3-GFP particle. The yellow asterisk shows the first nascent MT undergoing catastrophe. The red line indicated by the yellow arrowhead shows the persistence residence of the AUG3-GFP. The scale bar represents 2 μm.

(D) Distribution of five designated types of events, illustrating the relationship between augmin/γTuRC (red dots) dynamicity and MT (green lines) nucleation. Respective numbers of AUG3-GFP, AUG7-GFP, and GCP2-3xGFP particles were quantified, and the numbers were converted to percentages in each category, with the SD of the mean in each category representing the variation among the cells used in the quantification. MT nucleation events at MT crossover sites were included in the calculation and were incorporated into either branching or parallel nucleation, accordingly. Error bars indicate SD.

See also Figures S1–S3 and Movies S1 and S2.

of them led to de novo MT nucleation (type 5 in Figure 1D; Figure S2B; Movie S1). These results were similar to the data gathered from the hypocotyl cells [8]. In contrast, only 2 out of 1,149 AUG3/7 particles appeared at cortical sites devoid of MTs, and de novo nucleation was never detected (Figure 1D). Therefore, we concluded that augmin specifically regulates MT-dependent MT nucleation in interphase cortical MTs.

Branched MT nucleation was first described as "microtubular fir-trees" inside the gigantic spindle apparatus in *Haemanthus* endosperm [22]. Such a nucleation pattern is now recognized to be shared by animal cells and recapitulated by electron microscopy [14, 23]. The augmin complex interacts with the γTuRC and likely recruits the latter to MT walls to initiate branching nucleation with shallow angles (<30°); such a nucleation event has been reconstituted in vitro using frog egg extracts [24]. However, this nucleation event still lacks in vivo evidence that links MT nucleation with the residence of augmin. Our earlier findings have reached similar conclusions in plant cells undergoing mitosis as well [16]. The live-cell imaging data presented here further provided the most convincing evidence that augmin is involved in MT-dependent MT nucleation on interphase cortical MTs in living plant cells. Interestingly, a recent study showed that the γTuRC that is recruited to the mitotic spindle by augmin is not stably fixed at the initial location but sorted poleward by motor proteins [25]. However, the augmin complex and γTuRC were immobilized once being attached to the wall of cortical MTs. Therefore, interphase plant cells might employ additional anchoring proteins that immobilize augmin and γTuRC at the initial landing sites on the extant MTs.

Augmin Colocalizes with the γTuRC in Interphase Cells

Augmin subunits colocalize with those of the γTuRC in mitotic cells, as demonstrated in *Arabidopsis* [15, 16]. To further investigate the relationship between the augmin complex and the γTuRC in interphase cells, we coexpressed AUG1-2xTagRFP and GCP3-GFP under the control of their native promoters. We observed that AUG1-2xTagRFP particles were overwhelmingly colocalized with GCP3-GFP particles in leaf epidermal cells (Figure 2A; Movie S3). The colocalization was further validated by time-lapse illustration and kymograph analysis (Figures 2B and 2C). Among 405 AUG1-2xTagRFP particles and 399 GCP3-GFP particles detected in four cells, 332 of each were colocalized, accounting for 82.0% of AUG1-2xTagRFP and 83.2% of GCP3-GFP (Figure 2D; Movie S3). The GCP3-GFP particles that did not colocalize with

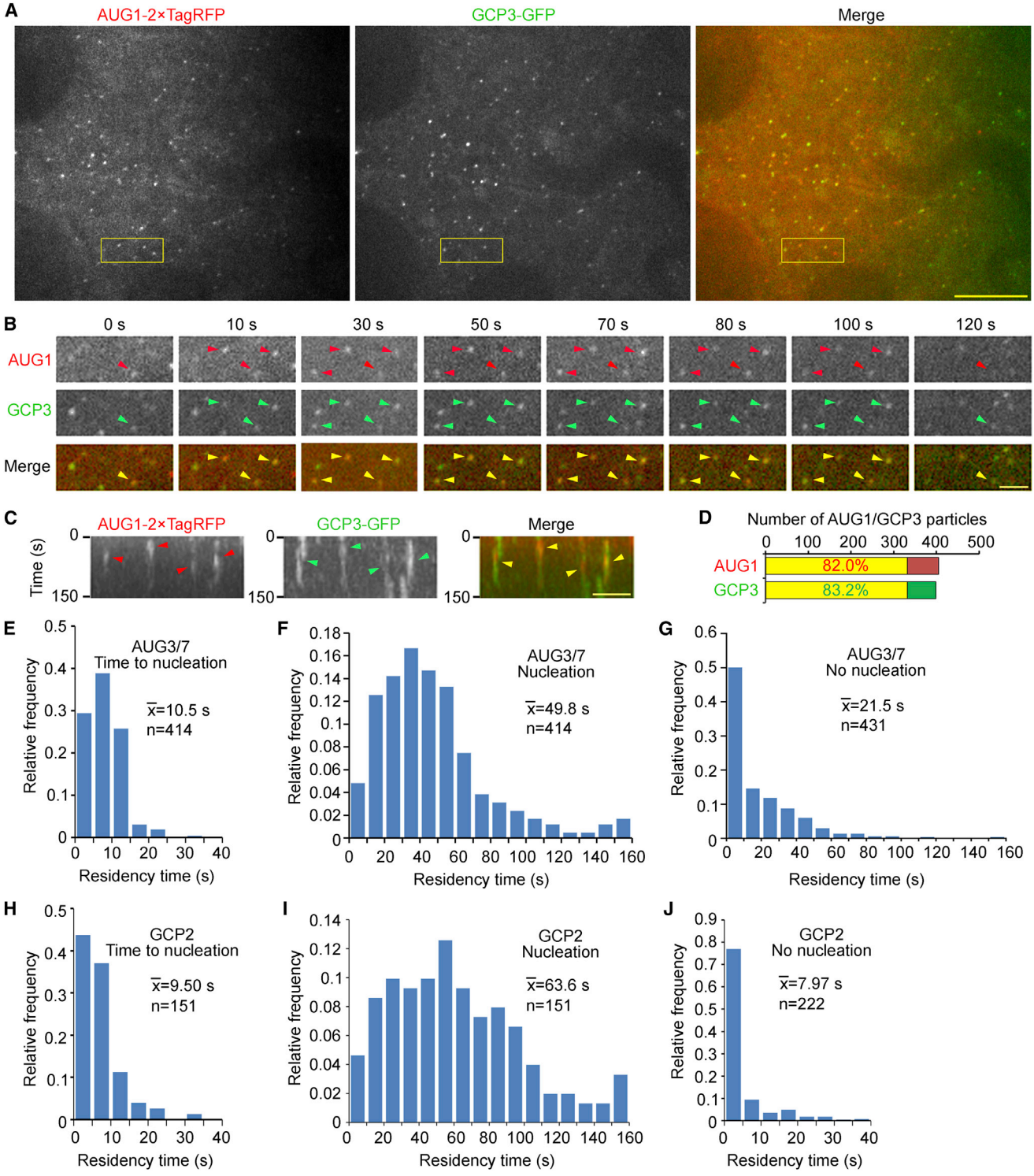

Figure 2. Colocalization of the Augmin Complex and the γ-Tubulin Complex in Interphase Pavement Cells

(A–C) The AUG1-2xTagRFP signal overlaps with that of GCP3-GFP at the cell cortex in epidermal pavement cells (A). Scale bar represents 10 μm. The yellow boxes highlight the area used for time-lapsed illustration in (B) and for kymograph analysis in (C). Arrowheads indicate particles showing colocalization. Scale bars of (B) and (C) represent 2 μm. See also Movie S3.

(D) Quantitative analysis of the proportion of colocalization, indicated in yellow in the histogram, between AUG1-2xTagRFP (in red) and GCP3-GFP (in green).

(E) Distribution of the times required for new MT initiation after AUG3/7-GFP particles were recruited to the MTs, as shown in Figure 1D.

(F) Distribution of the residency times of AUG3/7-GFP particles associated with MT nucleation, as shown in Figure 1D.

(G) Distribution of the residency times of AUG3/7-GFP particles which did not lead to new MT initiation, as shown in Figure 1D.

(H) Distribution of the times required for new MT initiation after GCP2-3xGFP particles were recruited to the MTs, as shown in Figure 1D.

(I) Distribution of the residency times of GCP2-3xGFP particles associated with MT nucleation, as shown in Figure 1D.

(J) Distribution of the residency times of GCP2-3xGFP particles which did not lead to new MT initiation, as shown in Figure 1D.

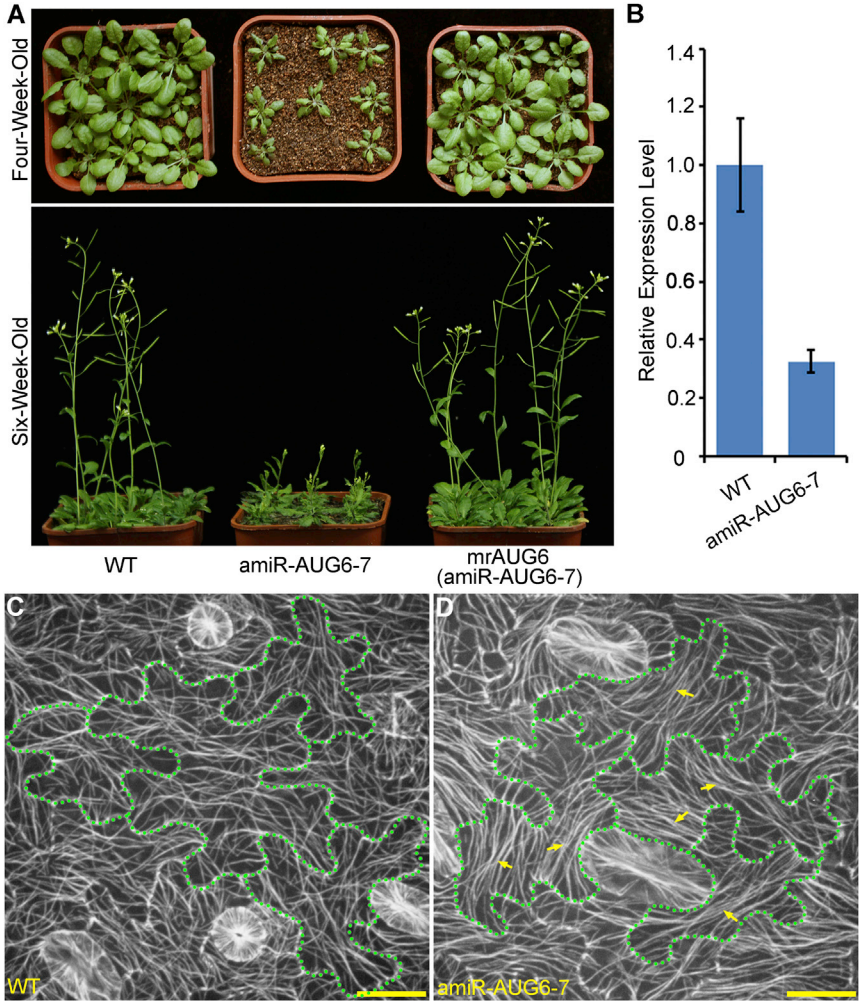

Figure 3. Severe Growth Retardation and Parallel Cortical MT Arrays in *AUG6* Knockdown Lines

(A) Downregulation of *AUG6* caused severe growth retardation, which was rescued by introducing a miRNA-resistant construct (mrAUG6). Top: 4-week-old plants; Bottom: 6-week-old plants. The wild-type plants are on the left, the amiR-AUG6-7 lines are in the middle, and the rescued lines are on the right.

(B) Assessment of *AUG6* expression in the amiR-AUG6-7 line by quantitative real-time PCR. Error bars indicate SD.

(C and D) A maximum Z projection of the image series showing fine cortical MT network in epidermal cells of the wild-type plants (C) and overall well-aligned MT arrays (indicated by yellow arrows) in the amiR-AUG6-7 cells (D). Green dashed lines highlight cell outlines of the epidermal cells. The scale bars represent 20 μm.

AUG1-2xTagRFP might represent a subpopulation of γTuRC that was transiently recruited to cortical sites (e.g., on the plasma membrane) devoid of MTs. As expected, the average residency time of GCP3-GFP particles showing noncolocalized pattern was 36.8 s, in contrast to 55.0 s for those particles showing colocalization. Furthermore, we calculated the time from the arrival of GFP-labeled augmin or γTuRC particles on the MTs to the start of nucleation and the lifespan of augmin or γTuRC particles (Figures 2E–2J). Compared to the γTuRC, a bit more time was required for augmin to initiate MT nucleation (Figures 2E and 2H), indicating that the augmin appeared a little bit earlier than the γTuRC. In contrast, the lifespan of augmin associated with MT nucleation was shorter than that of the γTuRC (Figures 2F and 2I), indicating that the augmin detached from the nascent MTs earlier than the γTuRC, which still end capped the minus ends of the nascent MTs. Collectively, these findings support the notion that augmin functions in recruiting γTuRC to initiate MT-dependent MT nucleation.

Impairment of Augmin Function Severely Suppresses MT Nucleation and Alters Cortical MT Organization

To examine how MT nucleation might be affected when the function of augmin was impaired, we generated augmin knockdown lines by expressing an artificial microRNA (miRNA) targeted at *AUG6* (amiR-AUG6). The transgenic lines, as represented here by the amiR-AUG6-7 line, showed severe growth retardation, with reduced leaf sizes and seedling dwarfism albeit being fertile (Figure 3A), with the AUG6 expression level reduced to 32.5% of that in the control (Figure 3B). The growth retardation phenotype was confirmed to be specifically caused by amiR-AUG6 because introducing a miRNA-resistant version of *AUG6* into the knockdown line restored growth to a level indistinguishable from that of the wild-type control (Figure 3A). Strikingly, cortical MTs in the amiR-AUG6 pavement cells became highly ordered parallel bundles, in contrast to the fine MT network in wild-type cells (Figures 3C and 3D).

To further determine how cortical MTs achieved such a configuration in the amiR-AUG6 cells, we analyzed MT nucleation patterns and frequencies when comparing to wild-type cells (Figures 4A and 4B) by applying the walking image subtraction approach modified from a published method [26]. This method allowed us to precisely discern both branching and parallel nucleation patterns and distinguish them from MT rescue events (Figure S4; Movie S4), and it led us to determine a frequency of MT nucleation at 62.8 events per 100 μm^2 per hour (n = 381, 9 cells) in wild-type pavement cells (Figure 4C), which was consistent with previously reported 57.7 events per 100 μm^2 per hour in the same cell type [27]. However, in amiR-AUG6 cells, the nucleation frequency was reduced to 9.16 events per 100 μm^2 per hour (n = 187, 15 cells) (Figure 4C). Both branching and parallel nucleation forms were suppressed in amiR-AUG6 cells. Specifically, the branching nucleation represented approximately 82.3% of the total nucleation events in wild-type cells, and the rest (17.7%) were parallel nucleation events. In amiR-AUG6 cells, however, the parallel MT nucleation prevailed and accounted for 63.4%, and the rest (36.6%) were branching nucleation (Figures 4D and 4E). We also found that in branching MT nucleation events, the branching angles in amiR-AUG6 cells were reduced to 29.7° ± 10.5°, compared to 41.0° ± 12.6° found in wild-type cells (Figures 4D and 4E).

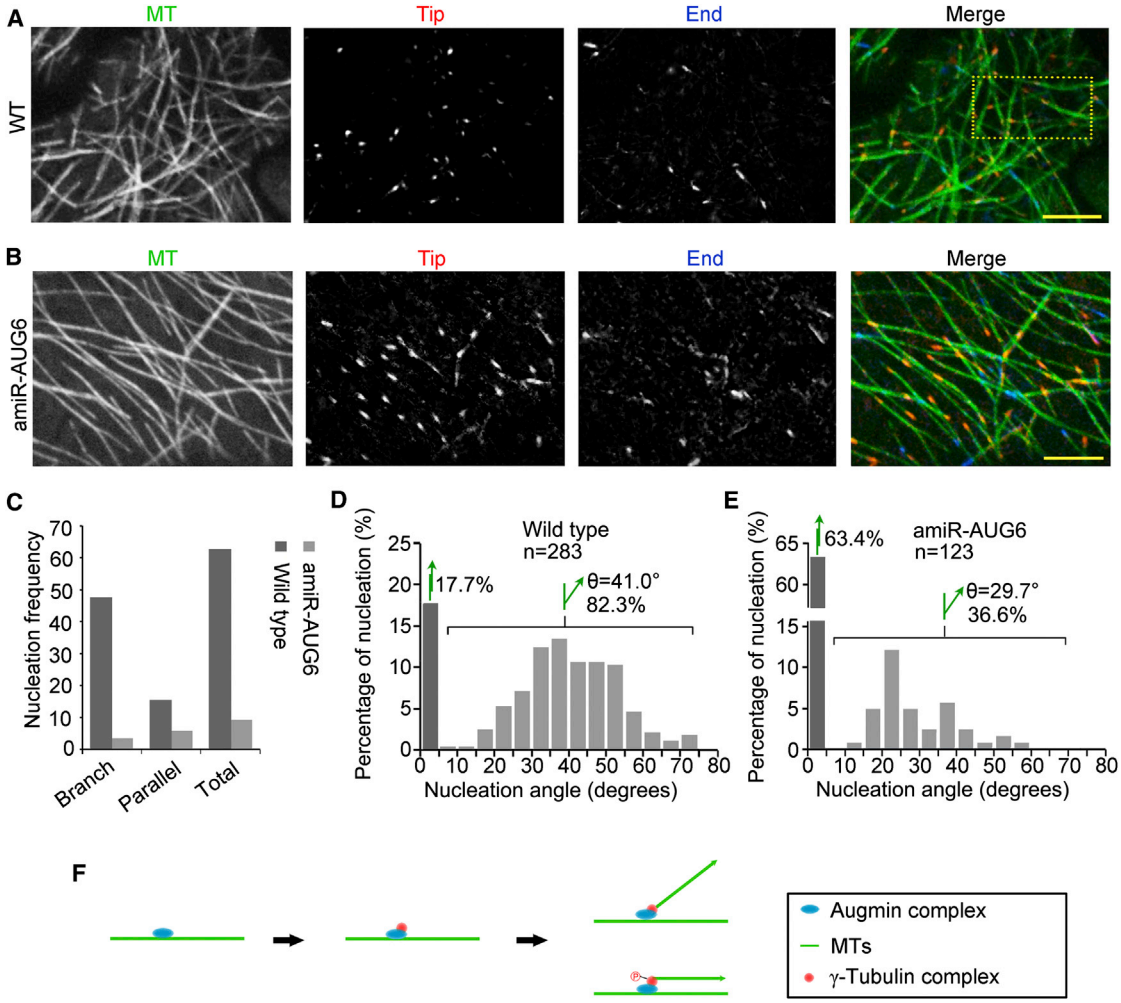

Figure 4. Altered MT Nucleation Behaviors in *AUG6* Knockdown Cells

(A and B) Cortical MTs and accompanying growing tips and shrinking ends in pavement cell of the wild-type (A) and the amiR-AUG6-7 (B) line. A three-frame walking subtraction method was used to generate new image series (see Supplemental Experimental Procedures for details). In the merged images, MTs are highlighted in green, the growing tips are highlighted in red, and the shrinking ends are highlighted in blue. The dotted yellow box in the right panel in (A) highlights the area used for time-lapsed illustration in Figure S4 and Movie S4. Scale bars represent 5 μm.

(C) Comparison of the nucleation frequency between the amiR-AUG6-7 pavement cells and the wild-type control.

(D and E) Distribution of nucleation angles in the wild-type control (D) and the amiR-AUG6-7 pavement cells (E). The proportion of branching nucleation (light gray bars) and parallel nucleation (dark gray bars) was highlighted above the histogram(s). The average nucleation angle for branching nucleation was shown above the brackets.

(F) Model for augmin-triggered MT-dependent MT nucleation on cortical MTs. The augmin complex localizes to the sidewall of preexisting MTs, recruits the γ-Tubulin complex there, and initiates MT nucleation either in the branching form or in the parallel form. The circled P indicates posttranslational modifications, such as phosphorylation, which may lead to a parallel nucleation event.

Taken together, these results strongly indicate that the augmin complex plays a crucial role in MT-dependent MT nucleation for establishing the cortical MT network in interphase plant cells and that downregulation of augmin significantly altered MT nucleation patterns and reduced nucleation frequencies, most likely due to repressed recruitment of the MT nucleator γTuRC to preexisting MTs. To date, MT-dependent MT nucleation in interphase has only been noticed in plant cells. The critical function of augmin in this event might be considered to be a plant-exclusive phenomenon. However, an earlier report in animal cells also showed that downregulation of augmin led to highly bundled and compact interphase MTs that encircled the nucleus instead of having their plus ends extend toward the cell periphery [28]. A unified mechanism may lie behind the organization of interphase MTs in plant and animal cells.

Conclusions

In this study, we uncovered a mechanism by which the augmin complex governed MT-dependent MT nucleation in interphase plant cells. We proposed that the augmin complex was recruited to cortical MTs via a yet-unknown mechanism and then allowed the γTuRC to be docked in order to initiate a nucleation event in respective patterns (see the model in Figure 4F). To our knowledge, the data presented here provide the most convincing evidence that supports augmin being a bridging factor and probably the recruitment factor of the γTuRC during MT-dependent MT nucleation for organizing interphase cortical MTs. Future work should be aimed not only at identifying novel partners (anchoring proteins or adaptors) that interact with the augmin complex but also at exploring novel regulatory events that specify various nucleation forms.

Supplemental Information

Supplemental Information includes Supplemental Experimental Procedures, four figures, and four movies and can be found with this article online at http://dx.doi.org/10.1016/j.cub.2014.09.053.

Author Contributions

Z.K., B.L., G.X., and J.T. conceived the study and designed the experiments. T.L., J.T., and C.W. performed most of the experiments. Y.Y., Y.M., and X.Z. provided assistance in the experiments. G.W., T.L., and Z.K. analyzed the data and assembled the figures and movies. G.W. developed the program for time-lapsed walking subtraction processing in MATLAB. Z.K., B.L., and G.X. wrote the paper.

Acknowledgments

We thank Takashi Hashimoto at the Nara Institute of Science and Technology for generously providing the GCP2-3xGFP, GCP3-GFP, and mCherry-TUB6 lines. We also thank Lei Jiao, Meng Lai, and Colin Hornby at Perkin Elmer for the technical support of the UltraView Vox system. This study was supported by the National Science Foundation of China under grant #31171294, by the startup fund of "One Hundred Talents" program of the Chinese Academy of Sciences to Z.K., and by the National Science Foundation under grant #MCB-1243959 to B.L.

Received: July 14, 2014
Revised: September 4, 2014
Accepted: September 22, 2014
Published: October 30, 2014

References

1. Lloyd, C., and Chan, J. (2008). The parallel lives of microtubules and cellulose microfibrils. Curr. Opin. Plant Biol. *11*, 641–646.
2. Paredez, A.R., Somerville, C.R., and Ehrhardt, D.W. (2006). Visualization of cellulose synthase demonstrates functional association with microtubules. Science *312*, 1491–1495.
3. Ehrhardt, D.W. (2008). Straighten up and fly right: microtubule dynamics and organization of non-centrosomal arrays in higher plants. Curr. Opin. Cell Biol. *20*, 107–116.
4. Shaw, S.L. (2013). Reorganization of the plant cortical microtubule array. Curr. Opin. Plant Biol. *16*, 693–697.
5. Wasteneys, G.O., and Ambrose, J.C. (2009). Spatial organization of plant cortical microtubules: close encounters of the 2D kind. Trends Cell Biol. *19*, 62–71.
6. Li, S., Lei, L., Somerville, C.R., and Gu, Y. (2012). Cellulose synthase interactive protein 1 (CSI1) links microtubules and cellulose synthase complexes. Proc. Natl. Acad. Sci. USA *109*, 185–190.
7. Murata, T., Sonobe, S., Baskin, T.I., Hyodo, S., Hasezawa, S., Nagata, T., Horio, T., and Hasebe, M. (2005). Microtubule-dependent microtubule nucleation based on recruitment of gamma-tubulin in higher plants. Nat. Cell Biol. *7*, 961–968.
8. Nakamura, M., Ehrhardt, D.W., and Hashimoto, T. (2010). Microtubule and katanin-dependent dynamics of microtubule nucleation complexes in the acentrosomal Arabidopsis cortical array. Nat. Cell Biol. *12*, 1064–1070.
9. Chan, J., Sambade, A., Calder, G., and Lloyd, C. (2009). Arabidopsis cortical microtubules are initiated along, as well as branching from, existing microtubules. Plant Cell *21*, 2298–2306.
10. Hashimoto, T. (2013). A ring for all: γ-tubulin-containing nucleation complexes in acentrosomal plant microtubule arrays. Curr. Opin. Plant Biol. *16*, 698–703.
11. Goshima, G., Mayer, M., Zhang, N., Stuurman, N., and Vale, R.D. (2008). Augmin: a protein complex required for centrosome-independent microtubule generation within the spindle. J. Cell Biol. *181*, 421–429.
12. Lawo, S., Bashkurov, M., Mullin, M., Ferreria, M.G., Kittler, R., Habermann, B., Tagliaferro, A., Poser, I., Hutchins, J.R., Hegemann, B., et al. (2009). HAUS, the 8-subunit human Augmin complex, regulates centrosome and spindle integrity. Curr. Biol. *19*, 816–826.
13. Uehara, R., Nozawa, R.S., Tomioka, A., Petry, S., Vale, R.D., Obuse, C., and Goshima, G. (2009). The augmin complex plays a critical role in spindle microtubule generation for mitotic progression and cytokinesis in human cells. Proc. Natl. Acad. Sci. USA *106*, 6998–7003.
14. Goshima, G., and Kimura, A. (2010). New look inside the spindle: microtubule-dependent microtubule generation within the spindle. Curr. Opin. Cell Biol. *22*, 44–49.
15. Ho, C.M., Hotta, T., Kong, Z., Zeng, C.J., Sun, J., Lee, Y.R., and Liu, B. (2011). Augmin plays a critical role in organizing the spindle and phragmoplast microtubule arrays in Arabidopsis. Plant Cell *23*, 2606–2618.
16. Hotta, T., Kong, Z., Ho, C.M., Zeng, C.J., Horio, T., Fong, S., Vuong, T., Lee, Y.R., and Liu, B. (2012). Characterization of the Arabidopsis augmin complex uncovers its critical function in the assembly of the acentrosomal spindle and phragmoplast microtubule arrays. Plant Cell *24*, 1494–1509.
17. Johmura, Y., Soung, N.K., Park, J.E., Yu, L.R., Zhou, M., Bang, J.K., Kim, B.Y., Veenstra, T.D., Erikson, R.L., and Lee, K.S. (2011). Regulation of microtubule-based microtubule nucleation by mammalian polo-like kinase 1. Proc. Natl. Acad. Sci. USA *108*, 11446–11451.
18. Zhu, H., Coppinger, J.A., Jang, C.Y., Yates, J.R., 3rd, and Fang, G. (2008). FAM29A promotes microtubule amplification via recruitment of the NEDD1-gamma-tubulin complex to the mitotic spindle. J. Cell Biol. *183*, 835–848.
19. Zeng, C.J., Lee, Y.R., and Liu, B. (2009). The WD40 repeat protein NEDD1 functions in microtubule organization during cell division in Arabidopsis thaliana. Plant Cell *21*, 1129–1140.
20. Wu, G., Lin, Y.T., Wei, R., Chen, Y., Shan, Z., and Lee, W.H. (2008). Hice1, a novel microtubule-associated protein required for maintenance of spindle integrity and chromosomal stability in human cells. Mol. Cell. Biol. *28*, 3652–3662.
21. Nakamura, M., Yagi, N., Kato, T., Fujita, S., Kawashima, N., Ehrhardt, D.W., and Hashimoto, T. (2012). Arabidopsis GCP3-interacting protein 1/MOZART 1 is an integral component of the γ-tubulin-containing microtubule nucleating complex. Plant J. *71*, 216–225.
22. Bajer, A.S., and Molè-Bajer, J. (1986). Reorganization of microtubules in endosperm cells and cell fragments of the higher plant Haemanthus in vivo. J. Cell Biol. *102*, 263–281.
23. Kamasaki, T., O'Toole, E., Kita, S., Osumi, M., Usukura, J., McIntosh, J.R., and Goshima, G. (2013). Augmin-dependent microtubule nucleation at microtubule walls in the spindle. J. Cell Biol. *202*, 25–33.
24. Petry, S., Groen, A.C., Ishihara, K., Mitchison, T.J., and Vale, R.D. (2013). Branching microtubule nucleation in Xenopus egg extracts mediated by augmin and TPX2. Cell *152*, 768–777.
25. Lecland, N., and Lüders, J. (2014). The dynamics of microtubule minus ends in the human mitotic spindle. Nat. Cell Biol. *16*, 770–778.
26. Lindeboom, J.J., Nakamura, M., Hibbel, A., Shundyak, K., Gutierrez, R., Ketelaar, T., Emons, A.M., Mulder, B.M., Kirik, V., and Ehrhardt, D.W. (2013). A mechanism for reorientation of cortical microtubule arrays driven by microtubule severing. Science *342*, 1245533.
27. Kirik, A., Ehrhardt, D.W., and Kirik, V. (2012). TONNEAU2/FASS regulates the geometry of microtubule nucleation and cortical array organization in interphase Arabidopsis cells. Plant Cell *24*, 1158–1170.
28. Hughes, J.R., Meireles, A.M., Fisher, K.H., Garcia, A., Antrobus, P.R., Wainman, A., Zitzmann, N., Deane, C., Ohkura, H., and Wakefield, J.G. (2008). A microtubule interactome: complexes with roles in cell cycle and mitosis. PLoS Biol. *6*, e98.